PCCP

Cite this: *Phys. Chem. Chem. Phys.*, 2011, **13**, 6544–6551

www.rsc.org/pccp

PAPER

Resonant inelastic X-ray scattering and X-ray absorption spectroscopy on the negative electrode material $Li_{0.5}Ni_{0.25}TiOPO_4$ in a Li-ion battery

H. M. Hollmark,*[a] K. Maher,[b] I. Saadoune,[b] T. Gustafsson,[c] K. Edström[c] and L.-C. Duda[a]

Received 25th November 2010, Accepted 15th February 2011
DOI: 10.1039/c0cp02668a

We have studied the first lithiation/delithiation cycle of the Li-ion battery electrode material $Li_xNi_{0.25}TiOPO_4$ applying X-ray absorption spectroscopy (XAS) and resonant inelastic X-ray scattering (RIXS). A set of ten identical $Li_xNi_{0.25}TiOPO_4$ battery electrodes have been cycled and left in different states of charge in the range of $x = 0.5 \ldots 2.5$, before disassembly in an Ar filled glove box. We find that Ni-, Ti-, and O-ions are affected simultaneously, rather than sequentially, upon lithiation of the material. In particular, Ni is reduced from Ni^{2+} to Ni^0 but only partially re-oxidized to Ni^{1+}, again, by delithiation. Overall, there is considerable "crosstalk" between the different atomic species and non-linearity in the response of the electronic structure during the lithiation/delithiation process. Fortuitously, the background variation in Ni L-XAS shows to contain valuable information about solid–electrolyte interface (SEI) creation, showing that the SEI is a function of the degree of lithiation.

1. Introduction

Since the introduction of Li battery (and nowadays Li-ion battery) technology there has been an enormous increase of research and development of these energy storage devices. Today, Li-ion batteries are found in a wide range of products—from mobile phones to power tools—and their importance for society is incontrovertible. Thus, in a market that continuously demands higher and higher energy outputs from Li-ion batteries, a vigorous search for novel, improved materials used in these devices has entailed.

So far $LiFePO_4$ has been the main candidate when it comes to $LiMPO_4$ (M = Fe, Mn, and Co) systems.[1–5] In an attempt to overcome the drawbacks of the $LiFePO_4$ material as high voltage materials for Li-ion battery electrodes, such as poor electrical conductivity and slow kinetics of lithium-ion diffusion, carbon coating and decreasing particle size have been employed. $LiMnPO_4$, $LiCoPO_4$, and $LiNiPO_4$ have also attracted interest lately, but they all suffer from the same drawbacks as $LiFePO_4$. Another attempt to improve the existing candidates has been made by creating solid solutions between different olivine structured $LiMPO_4$ systems.[6] Lately $Li_{0.5}Ni_{0.25}TiOPO_4$ has been suggested as a future candidate since it has a low cycling potential ($\approx$1.7 V) and a good capacity retention during cycling.[7]

There are open questions concerning the interplay of charge uptake between the metal ions among themselves as well as between the metal ions and the oxygen ions. For instance, it would be of great interest to clarify whether Ni or Ti changes its valence first, or if they change valence simultaneously during lithiation. In the material $Li_{0.5}Ni_{0.25}TiOPO_4$ we have Ni^{2+} and Ti^{4+}. Presently, it is considered that during the insertion of 1.5 Li-ions in the $Li_{0.5}Ni_{0.25}TiOPO_4$ structure, the valence number of Ni changes from Ni^{2+} to Ni, and the valence number of Ti consequently changes from Ti^{4+} to Ti^{3+}.[7] The calculated theoretical capacity of $Li_{0.5}Ni_{0.25}TiOPO_4$ is 225 mA h g^{-1}, but since the material shows an experimental capacity of about 300 mA h g^{-1} for the first lithiation, it is speculated that the formation of a solid–electrolyte interface (SEI) also contributes to the experimental capacity of the material during the first lithiation.[7] Further, it is claimed that Ti^{4+}/Ti^{3+} is the main active redox couple and that Ni^{2+}/Ni accompanies at a later stage in the lithiation curve.

A deeper understanding of the electronic structure of these materials may provide a guide for refining this class of materials. From the theoretical side, for instance, first principle calculations have been reported on several different $LiMPO_4$ systems,[8] showing good agreement between calculations and experimental data. Experimentally, it is a challenge to gain knowledge about the processes involved in intercalation and deintercalation of Li in complex materials such as $Li_{0.5}Ni_{0.25}TiOPO_4$. To our knowledge, very little spectroscopical measurements are reported and those that exist are all

[a] *Department of Physics and Astronomy, Uppsala University, Box 516, SE-751 20, Uppsala, Sweden. E-mail: hakan.hollmark@physics.uu.se*
[b] *ECME, FST Marrakech, University Cadi Ayyad, BP549, Av. A. Khattabi, Marrakech, Morocco*
[c] *Department of Materials Chemistry, Uppsala University, Box 538, SE-751 21 Uppsala, Sweden*

powder and single crystal X-ray diffraction measurements.[9,10] A photoelectron spectroscopy study from the related material TiO_2 has shown that TiO_2 reduces about 32% of its Ti^{4+}-ions to a Ti^{3+} state during Li insertion, and that the binding energy for the lithiated material is lowered by as much as 2.1 eV.[11]

In this report, we present a systematic investigation of the first lithiation/delithiation cycle of $Li_xNi_{0.25}TiOPO_4$ using a combination of X-ray absorption spectroscopy (XAS) and resonant inelastic X-ray scattering (RIXS) in the soft X-ray range. We show that this is a powerful way to extract details about the chemical and symmetry dependent electronic structure of this material as a function of lithiation degree as achieved in a real, functioning battery. One key advantage is the insensitivity of photon-only spectroscopies to interfering surface contaminations that liquid electrolyte battery components are subject to. Since the oxidation states of the Ni and the Ti atoms are of great importance for the performance of the material we pay particular attention to this question in the XAS part of our study. By virtue of energy selective excitation, RIXS gives us a picture of the occupied partial (mainly 3d character for the metals and mainly 2p character for the oxygen) density of states (DOS) at inequivalent sites. This allows us to gain insight into the charge and energy distribution among the different sites of this complex material and the hybridization effects between metal and oxygen ions.

2. Experimental

2.1 Electrode and battery preparation

The cathode material $Li_{0.5}Ni_{0.25}TiOPO_4$ studied in this report was prepared by a co-precipitation method. A detailed description of the preparation method used is described in ref. 12. The electrodes were made from a mixture containing 75 wt% active material, 10 wt% super-P carbon powder, and 15% of PVDF [poly(vinylidene fluoride)] in NMP (1-methyl-2-pyrrolidinone). The mixture was applied onto an aluminium foil and dried for 6 h at 80 °C to remove the solvents. Circular electrodes were then cut from the aluminium foil and transferred into an argon-filled glove box (<1 ppm H_2O and O_2) and dried under vacuum at 120 °C overnight to remove water from the electrode material. A set of ten batteries (in foil welded plastic-covered aluminum pouches)[13] were assembled inside a glove-box. Lithium metal foil was used as counter electrode. As electrolyte a lithium salt, $LiPF_6$, dissolved in a mixture of ethylene carbonate and diethylcarbonate, EC : DEC (2 : 1 by volume), was used. The water in the electrolyte is <10 ppm, as determined by the Karl Fischer titration. A Cellguard separator was used to keep the electrodes apart and to prevent the cells from failing due to short circuit.

2.2 Electrochemical cycling

Ten battery cells were made, named C_0–C_9. Cell C_0 was left untouched after assembling the batteries, that is $x = 0.5$ in $Li_xNi_{0.25}TiOPO_4$. Lithiation and delithiation were performed for all samples at a rate of C/20. During the lithiation (intercalation), cells C_1–C_6 were stopped at different x-values between 0.6 to 2.5, and in the same manner the cells C_7–C_9 were stopped at different x-values during the delithiation (deintercalation). Fig. 1 shows where in the lithiation/delithiation curve the different cells have been stopped. Mass, current, and charge for each cell are shown in Table 1. Note that in the delithiation process it is not possible to extract all the extra Li-ions from the lithiation process. At maximal delithiation $x = 1.25$, *i.e.* a state corresponding to the lithium content achieved between C_2–C_3 of the lithiation process.

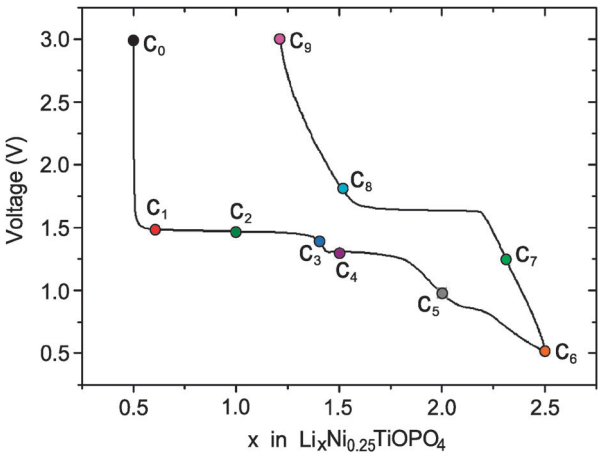

Fig. 1 The lithiation/delithiation curve for $Li_xNi_{0.25}TiOPO_4$. The dots indicate where on the curve the different cells are stopped.

Table 1 (from left to right) The different Li contents (x) for cells C_0–C_9, the mass of the active material in the cells, the current used for cycling the cells, and lastly the charges passed through the cell to reach the specific x-value of each cell

Cell	x	Mass/mg	Current, I/mA	Charge, Q/mA h
C_0	0.5	6.2673	—	—
C_1	0.6	6.4275	0.04866	0.09732
C_2	1.0	5.1375	0.03889	0.3889
C_3	1.4	4.4025	0.03333	0.5994
C_4	1.5	6.7575	0.05116	1.0232
C_5	2.0	5.7600	0.04361	1.3083
C_6	2.5	7.5000	0.05678	2.2712
C_7	2.3	6.3450	0.04804	2.2098
C_8	1.5	6.8775	0.05207	3.2804
C_9	1.25	7.2000	0.05445	3.7026

2.3 X-Ray spectroscopy

After cycling, we transferred the batteries into an Ar filled glove box, where they were kept for approximately 24 h before the pouch cell was opened. Then the electrodes were firmly attached onto a sample holder and transported to the synchrotron facility in an air-tight container. There the electrodes were transferred *via* a load lock into the measuring chamber of our home-built grazing incidence Rowland spectrometer.[14] The pressure in the measuring chamber was kept in the low 10^{-8} mbar region at all times.

The ten cells were investigated systematically with both X-ray Absorption Spectroscopy (XAS) and Resonant Inelastic X-ray Scattering (RIXS). XAS measurements were performed at the Ni L-, Ti L-, and O K-edge. For all edges both total fluorescence yield (TFY) and total electron yield (TEY) data were recorded during XAS. RIXS measurements were

performed at the Ni L-, Ti L-, and O K-edge using a laboratory built grazing incidence Rowland spectrometer.[14]

The measurements were performed at beamline U41-PGM[15] of BESSY II in Berlin, Germany. This is an undulator beamline with a flux density at the end-station of $<10^{12}$–10^{13} photons s^{-1} in the excitation energy interval 170–1500 eV. The exit slit from the monochromator was set at 20 μm for XAS resulting in a resolution of 171 meV at the O K-edge (530 eV). For RIXS measurements the exit slit was set at 100 μm resulting in a resolution of 855 meV at the O K-edge (530 eV).

3. Results and discussion

3.1 Ni L-edge

In Fig. 2 we show XAS spectra at the Ni L-edge using TFY. Ni L-edge XAS is due to 2p → 3d transitions, which are characterized by a splitting of about 17.3 eV into the $2p_{3/2}$-edge (L_{III}) and the $2p_{1/2}$-edge (L_{II}), where the L_{II}-edge is weaker due to the statistical branching ratio (1 : 2). The $L_{III,II}$-edges are further split up into atomic multiplets, which is characteristic of the ionization state ("fingerprint")[16] featuring the main Ni L_{III} resonance at 849.5 eV.

We find that the lithiation process transforms the Ni-ions from an approximate Ni^{2+}-state at C_0 to a Ni^{1+} at an x-value close to 2.0 (between points C_4 and C_5 in Fig. 1). Further lithiation leads to Ni in a valence state of Ni^{1+}, or even somewhat below Ni^{1+} at $x = 2.5$ (C_6), which we deduce from the disappearance of the satellite of the main Ni peak. Subsequent delithiation (C_7–C_9) does not reverse this transformation completely, as the satellite peak only develops as a weak "shoulder". At maximal delithiation Ni is only oxidized back to a state corresponding to C_5 ($x \approx 2.0$), which is a much smaller oxidation than suggested by the electrochemical curve ($x \approx 1.25$) (Fig. 1 and Table 1).

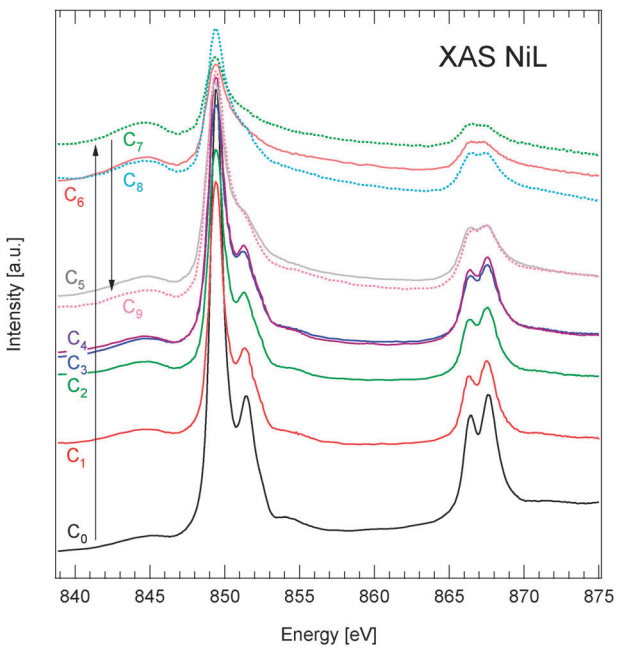

Fig. 2 XAS on $Li_xNi_{0.25}TiOPO_4$ at the Ni L-edge with different degrees of lithiation (x-value).

We point out that the spectra shown in Fig. 2 have only been normalized to the incident flux, I_0. Therefore the vertical offsets of the spectra shown in Fig. 2 are solely due to a (virtually structureless) background that varies as a function of lithiation degree, with an increasing background from C_0 to C_6 in the course of the lithiation (solid lines). The highest background is found in sample C_7, which means that there is some hysteresis in the effect on the background. The maximally delithiated sample, C_9, retains a background intensity very similar to point C_5 during lithiation.

The constant part of the background is mostly an effect to C 1s-absorption from the carbon black and other carbon compound residues from incomplete removal of the electrolyte due to 3rd order light contamination of the monochromator. Note also that the broad peak that appears at approximately 5 eV below the main peak is a carbon absorption related feature. We propose that the variable part of the background is a sign for formation of a solid–electrolyte interface (SEI) on the electrode surfaces during cycling of the battery cells.

TEY measurements at the Ni L-edge (not presented), which are much more surface sensitive than TFY measurements, show a somewhat less systematic behavior regarding the background intensity. This is not surprising since there are various amounts of remnants from the electrolyte on the electrodes, possibly obscuring the signal from a SEI. Also, obvious from the TEY data is that for samples C_6 and C_7 the Ni signal was almost completely suppressed, indicating either a depletion of Ni in the surface of the electrode or a sufficiently thick residue to quench the Ni signal. The formation and composition of SEI on graphite electrodes has previously been studied with XAS and RIXS at the C K-edge,[17] suggesting that the SEI in that case was composed of lithium succinate, lithium methoxide and lithium oxalate.

In summary, the analysis of the Ni XAS-spectra has revealed some important details about the chemical processes of the first lithiation/delithiation cycle. Firstly, the dependence of the background signal on the degree of lithiation indicates that the background intensity most probably stems from a formation of a SEI on the electrodes during cycling of the battery cell. Secondly, this process is partially reversible as revealed by the decrease during subsequent delithiation. Thirdly, the SEI thickness correlates strongly with the Ni ionization state as seen by the similarity between the C_5- and C_9-spectra.

Results from RIXS experiments at the Ni L-edge on the studied material are shown in Fig. 3. We observe that the pristine electrode (C_0) shows a double structure (main peak and high-energy shoulder) that is characteristic for the e_g–t_{2g} crystal field splitting of Ni^{2+} excitations, *i.e.* dd-excitations. There is a systematic trend of a shift toward lower energy and also a decrease of the shoulder during intercalation between C_0 and C_5, with a total shift of about −0.35 eV. For sample C_6 there is an abrupt shift of about 0.65 eV back toward higher energy and the spectrum is symmetric without a high-energy shoulder. The subsequent charging (C_7–C_9) shows that the delithiation process is not able to reverse the entire lithiation process but leads to a state similar to the one of C_5 (Fig. 1).

In Fig. 4, RIXS at the Ni L-edge for samples C_0, C_2, C_5, C_6, and C_9 are shown. The spectra are normalized to the area

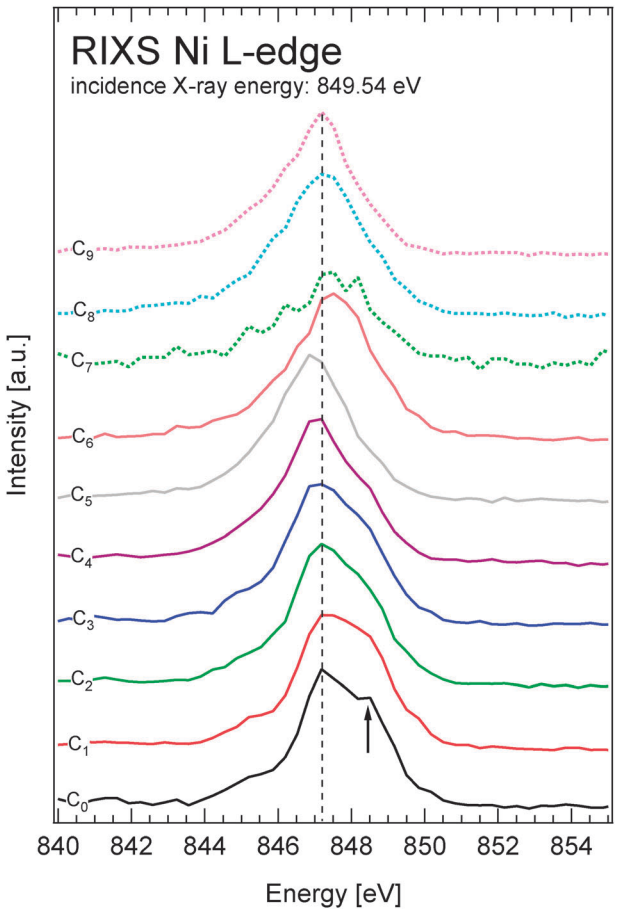

Fig. 3 RIXS on $Li_xNi_{0.25}TiOPO_4$ at the Ni L-edge with different degrees of lithiation (x-value). The spectra are normalized to the highest intensity for each spectrum. The excitation energy was 849.54 eV.

under the peak of the respective spectrum. When normalized in this fashion, it is revealed that the disappearance of the shoulder on the right hand side (denoted II in Fig. 4) of the peak during intercalation is accompanied by an increased intensity of the peak denoted I in Fig. 4, as seen for sample C_5. There appears to exist two different states for the Ni-ion and the spectra therefore group into a state as in C_0, C_1, C_2, C_3, C_4, and C_6 or into a state as in C_5, C_7, C_8, and C_9. A more detailed analysis of the line shapes reveals that the percentage of fully oxidized Ni drops to about 35% for C_5, only to abruptly rise to about 50% for C_6 and, upon delithiation, to gradually drop to 45% for C_9. Thus the delithiation only leads to a partial re-oxidation of Ni. This is probably due to an irreversible process that appears to take place between C_5 and C_6. This also correlates with the disproportionally strong increase between C_5 and C_6 seen in the background intensity of the Ni L-XAS spectra that we have discussed above.

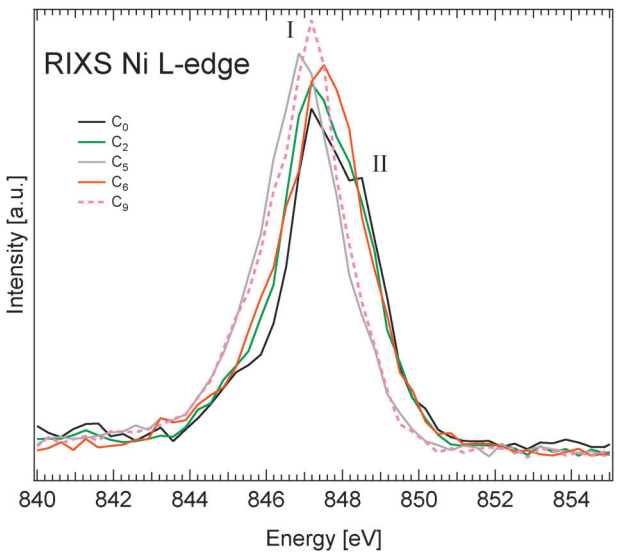

Fig. 4 RIXS on $Li_xNi_{0.25}TiOPO_4$ at the Ni L-edge with different degrees of lithiation (x-value). The spectra are normalized to the area under each spectrum. The excitation energy was 849.54 eV.

3.2 Ti L-edge

XAS at the Ti L-edge using TFY is shown in Fig. 5 where the L_{III}-(L_{II}-) resonances are found at energies below (above) 460 eV. The spectra show some resemblance to Ti L-edge XAS of Li_xTiO_2[18] as well as other d^0 compounds, such as $FeTiO_3$.[16] Note, however, that the crystal symmetry of $Li_xNi_{0.25}TiOPO_4$ differs from that of both TiO_2 and $FeTiO_3$. TiO_2 exists in several different phases, among them are anatase and rutile, where rutile is the most stable and common form. Anatase has D_{2d} crystal symmetry and rutile has D_{2h}

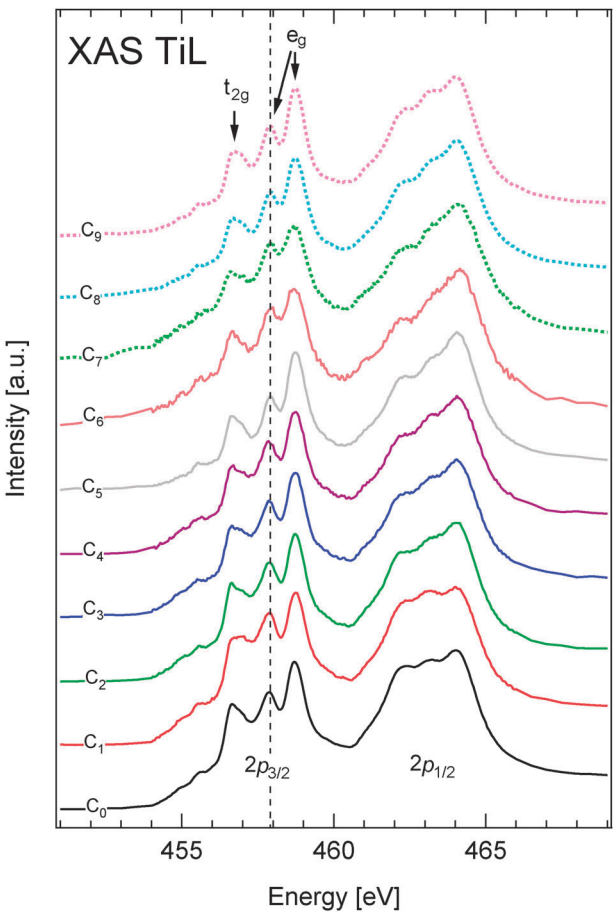

Fig. 5 XAS on $Li_xNi_{0.25}TiOPO_4$ at the Ti L-edge with different degrees of lithiation (x-value).

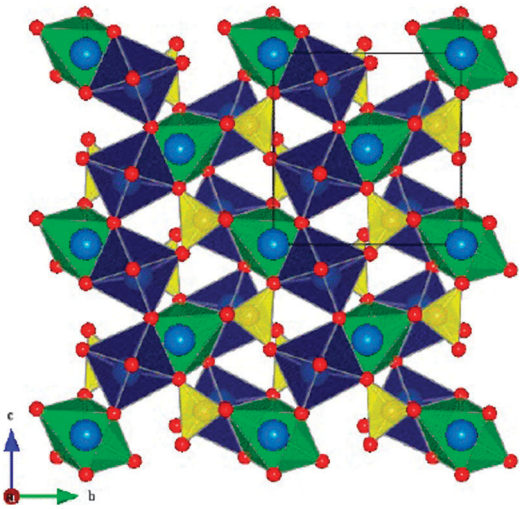

Fig. 6 The structure of $Li_xNi_{0.25}TiOPO_4$. P atoms are inside the yellow, Ti inside the dark blue, and Ni inside the green volumes. The O atoms are colored red and Li atoms light blue.

symmetry. Rutile can also be presented in D_{4h} or O_h symmetry,[16] even if computational difficulties arise when using O_h symmetry. In $Li_xNi_{0.25}TiOPO_4$, the Ni and Ti ions exist as NiO_6 and TiO_6 octahedra and are best presented in crystal symmetry C_{2h}, which is a monoclinic crystal system. Fig. 6 shows the structure of $Li_xNi_{0.25}TiOPO_4$.

Fig. 7 displays an enlarged part of the XAS spectra at the Ti L-edge for C_0, C_2, C_5, and C_9. We find that the lithiation/delithiation process mainly affects the intensity of the peaks a and b that belong to excitations into e_g- and t_{2g}-states, respectively. We see a general trend that charge insertion decreases the number of empty states (*i.e.* the XAS-intensity decreases) and *vice versa* for charge extraction. However, due to the complexity of the XAS multiplet structure it is less straightforward than for Ni XAS to determine the change of the Ti oxidation states more quantitatively. Moreover, in contrast to the case of TiO_2,[11,18] there is no visible shift of the XAS peaks toward lower energies during lithiation of $Li_xNi_{0.25}TiOPO_4$, hence making a determination of the oxidation state for Ti more difficult. Analogously to the Ni L-edge, but to a lesser extent, we see that the electrochemistry is not completely reversible for Ti. At maximal delithiation (C_9) Ti is only oxidized back to a state corresponding to C_3 ($x \approx 1.4$), which is a somewhat smaller oxidation than suggested by the electrochemical curve $x \approx 1.25$ (Fig. 1 and Table 1).

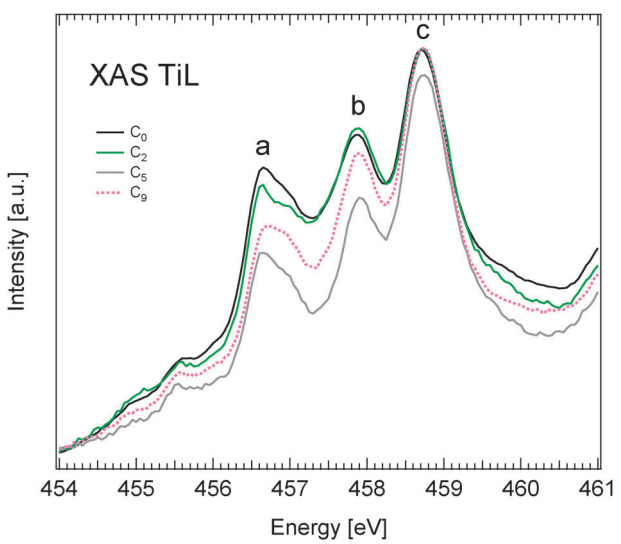

Fig. 7 XAS on $Li_xNi_{0.25}TiOPO_4$ at the Ti L-edge with different degrees of lithiation (x-value).

Ti L-edge RIXS spectra are shown in Fig. 8. There are three distinct peaks: the elastically scattered X-rays at 458.2 eV, a small peak (marked with a dashed line) at 457.5 eV corresponding to pure Ti 3d-band orbitals,[18] and a broad peak situated at approximately 451.5 eV reflecting the Ti orbitals heavily hybridized with O 2p-orbitals. The spectra are normalized with respect to the latter peak. The relative spectral weights of the pure Ti 3d-band peak vary considerably during the lithiation/delithiation process, reflecting the changes in occupation of this band. Initially (C_0), the band is empty and starts to fill up upon lithiation, reaching a maximum at around C_2. Further lithiation, surprisingly, depletes the Ti 3d-band again, whereby a minimum is observed at about C_5. Delithiation (C_7–C_9) leads to an increase of the spectral weight again, which at maximal delithiation (C_9) is similar as in C_4,

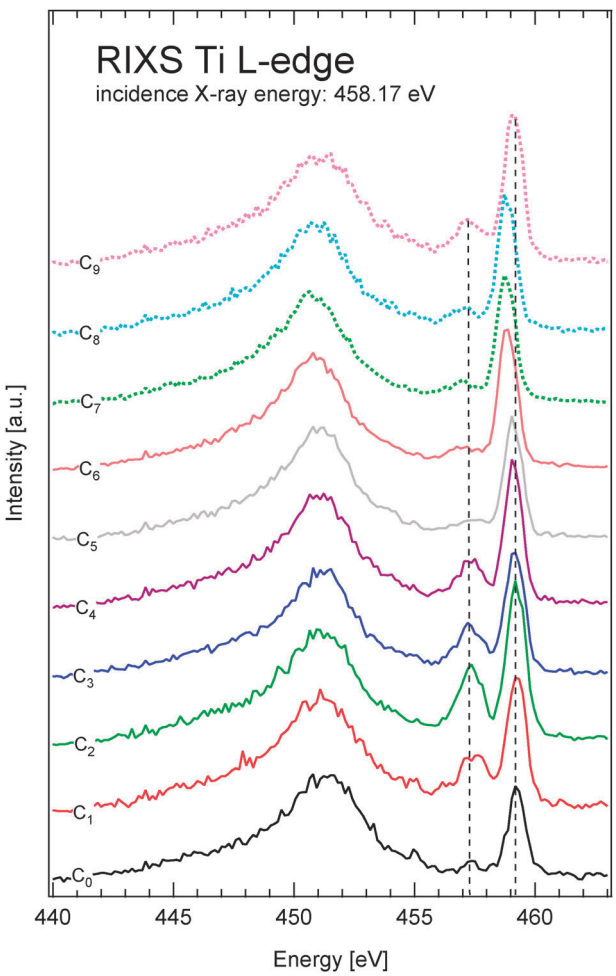

Fig. 8 RIXS on $Li_xNi_{0.25}TiOPO_4$ at the Ti L-edge with different degrees of lithiation (x-value). The spectra are normalized to the highest intensity for each spectrum. The excitation energy was 458.17 eV.

i.e. $x \approx 1.5$. This is close to the result from the analysis of the Ti L-XAS spectra $x \approx 1.4$.

3.3 O K-edge

Fig. 9 displays the XAS at the O K-edge using TFY, which reflects the unoccupied states in the O 2p-band. There is a large number of inequivalent oxygen atoms that bond to Ni, Ti, and P, giving rise to a complex XA-spectrum. It would be valuable to be able to assign the observed structures to their predominant hybridization character, in particular the bottom of the conduction band that corresponds to the low-energy peak at about 529.8 eV.

We start by describing the effect of lithiation and delithiation. Upon lithiation, the intensity of the peak at the bottom of the conduction band is found to decrease abruptly and to shift to lower energy by about 0.5 eV. The peak area does not change very much until excessive lithiation is reached, starting at C_5 and leading to almost complete suppression at C_6. Delithiation (C_7–C_9) reverses the change only incompletely, leaving the conduction band minimum in a state close to the one found between C_1 and C_2. The other notable change in the conduction band is found in a region between 534.5 eV and the low-energy flank of the peak at about 538.2 eV.

We also performed O K-XAS measurements (not shown) on the reference samples NiO and TiO_2, in order to allow comparison to $Li_xNi_{0.25}TiOPO_4$ and possibly assist peak assignment (by fingerprinting). By this, we may tentatively ascribe the two low-energy peaks at 529.8 eV and 532.3 eV (and thereby the bottom of the conduction band) to excitation to O 2p-orbitals hybridizing with the crystal field split Ti 3d e_g- and t_{2g}-orbitals. The spectral weight of excitations to Ni-hybridized O 2p-orbitals is expected to be much less (from our XAS measurements $\sim 1/2$) due to the low concentration of Ni in $Li_xNi_{0.25}TiOPO_4$. Judging from the NiO reference measurement we expect that the low-energy flank of the peak at 532.3 eV as well as the high-energy flank of the peak at 538.2 eV contains some Ni 3d-character. Note, however, that neither the energy positions of the salient features nor the spectral shapes coincide well enough to allow an absolutely conclusive result. Moreover, there should be contributions from hybridization with P in the spectrum.

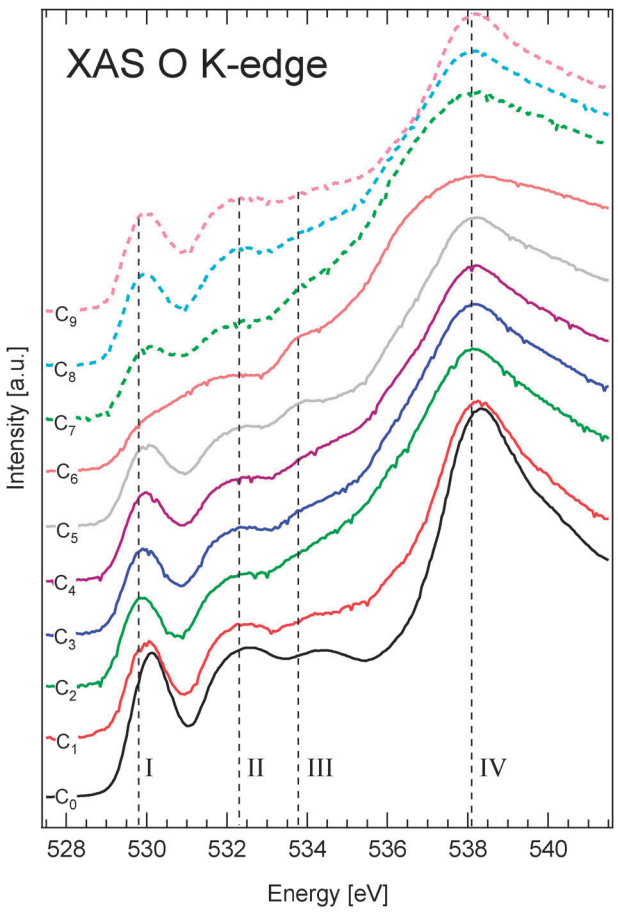

Fig. 9 XAS on $Li_xNi_{0.25}TiOPO_4$ at the O K-edge with different degrees of lithiation (x-value).

We performed RIXS measurements at incident energies (529.8 eV, 532.3 eV, 533.75 eV, and 538.1 eV) indicated by the dashed vertical lines. The results are shown in Fig. 10. There is a large change in the spectral shape between the oxygen RIXS spectra for the lowest incident energy (529.8 eV, denoted I) and the higher incident energies. At incident energy I we observe a single narrow peak. Initial lithiation leads to a further narrowing, reaching a minimum width for C_2 and further lithiation leads to a shift of the peak at −0.5 eV for C_6, as well as a pronounced high-energy shoulder around 526 eV. Delithiation does not reverse the process but first leads to a shift of 0.5 eV C_8 and then back by the same amount. The spectrum of the delithiated electrode C_9 thus resembles the situation achieved for C_6 except for the high-energy shoulder.

For the next incident energy (532.3 eV, denoted II), the oxygen spectra completely change appearance, reflecting either a change of symmetry or a change of site at the absorption peak. The spectra at the incident energy are much broader, with a large high-energy peak and a small low-energy peak, separated by about 4 eV. Lithiation and delithiation affect the spectral shape to some degree (but relatively less than for the lower incident energy), mostly characterized by a shift of the high-energy edge.

The spectra at next incident energy (533.75 eV, denoted III) resemble the situation achieved for incident energy II. Whereas at the highest incident energy, the spectra become even broader by a splitting of the large high-energy peak around 525 eV. The low-energy shoulder of this peak is very sensitive to the lithiation/delithiation process: initial lithiation (C_0–C_5) leads to a loss of spectral weight there and further lithiation (C_6) leads to a narrowing from the high-energy flank. Delithiation only leads to a partial restoration of the original situation, *i.e.* the peak broadens and the low-energy shoulder gains in spectral weight.

Note that we have tried to align the metal spectra to the oxygen spectra by correlating the charge transfer (CT) peak to the oxygen RIXS spectra (bottom panel in Fig. 10). By aligning the elastic peak observed for the Ti L-RIXS spectrum, we find that the Ti CT peak (at about −8.2 eV on the lower energy scale) coincides best with the sharp peak observed at the lowest incident energy. Furthermore, we align the tiny Ni CT peak with the Ti CT peak and find that the dd-peaks (at about −2 eV on the lower energy scale) overlap considerably, as expected. We observe no corresponding peak in the O

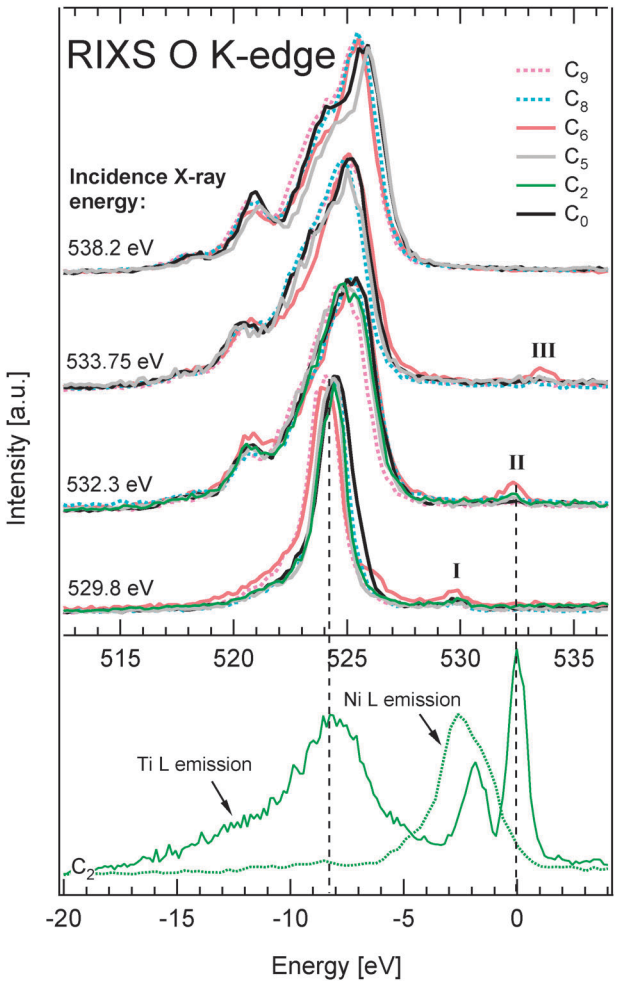

Fig. 10 RIXS on $Li_xNi_{0.25}TiOPO_4$ at the O K-edge with different degrees of lithiation (x-value). The spectra are normalized to the highest intensity for each spectrum, and the energy scale has been shifted to zero with respect to the elastic peak in the O K-edge RIXS spectra. The excitation energies were 529.8, 532.3, 533.75, and 538.2 eV respectively. The bottom two traces are Ni and Ti L-edge RIXS spectra included for comparison.

K-RIXS spectra as seen in some other 3d transition metal oxides[19–22] but this signature is usually rather weak.

In summary of this section, we may say that there is evidence that the conduction band minimum has large Ti character. The evolution of the oxygen spectra in the first lithiation/delithiation cycle corroborates our earlier findings that excessive lithiation (C_5–C_6) irreversibly changes the electronic structure of the $Li_xNi_{0.25}TiOPO_4$ battery cathode. This is most evident by inspection of the energy dependent O K-RIXS spectra, as described above.

4. Summary and conclusion

We have used XAS and RIXS to investigate $Li_xNi_{0.25}TiOPO_4$ as a Li-ion battery anode material for its first lithiation/delithiation cycle. The utility of the spectra can, to a large extent, be attributed to their ability of reflecting the partial density of states (occupied and unoccupied, respectively), especially for the oxygen edge. Moreover, in the case of Ni, we can quite accurately determine the change of the oxidation state for this ion.

For the lithiation process between $x = 0.5$ and $x = 2.5$, we find that Ni changes its oxidation state from Ni^{2+} ($x = 0.5$) to Ni^{1+} ($x = 2.0$) and finally to metallic Ni ($x = 2.5$). Delithiation of the material only incompletely reverses the changes from the lithiation process at Ni. Even for the maximally delithiated sample (C_9 in Fig. 1) Ni has only changed its valence number back to Ni^{1+}. We find intensity variations in the first two Ti L-XAS peaks during the first lithiation/delithiation cycle. Also the Ti ions show an incomplete reversal of the lithiation process. The Ti L-RIXS spectra clearly show how the Ti d-band receives and loses charge in the lithiation/delithiation process. It is, however, not a monotonic function of the degree of lithiation. Also the oxygen ions participate in the uptake of charge, but, in contrast to both Ni and Ti, this happens at a later stage in the lithiation (at $x \geq 1.5$).

Our results show that there exists considerable "crosstalk" between different atomic species, *i.e.* Ni, Ti, and O, regarding the response of the electronic structure to the lithiation/delithiation process. For this material, we must abandon the expected picture of a linear and sequential process in which a rigid band is filled up and emptied as a simple function of x. We conclude that Ni and Ti respond not sequentially, but simultaneously, to the lithiation/delithiation process. The irreversible changes that we found for the first cycle at the Ni-ion sites have, most likely, an inhibiting effect on subsequent battery cycles, especially suggesting a reduced activity of the Ni sites. Finally, we point out that our systematic investigation shows that the combination of XAS and RIXS is a powerful approach for extracting details of the lithiation process in complex TM-oxide Li-ion battery materials such as $Li_xNi_{0.25}TiOPO_4$.

References

1 A. K. Padhi, K. S. Nanjundaswamy and J. B. Goodenough, *J. Electrochem. Soc.*, 1997, **144**, 1188.
2 A. S. Andersson, J. O. Thomas, B. Kalska and L. Häggström, *Electrochem. Solid-State Lett.*, 2000, **3**, 66.
3 A. Yamada, S. C. Chung and K. Hinokuma, *J. Electrochem. Soc.*, 2001, **148**, A224.
4 S. Okada, S. Sawa, M. Egashira, J. I. Yamaki and M. Tabushi, *J. Power Sources*, 2001, **97–98**, 430.
5 D. D. MacNeil, Z. Lu, Z. Chen and J. R. Dahn, *J. Power Sources*, 2002, **108**, 8.
6 J. Wolfenstine and J. Allen, *J. Power Sources*, 2004, **136**, 150–153.
7 K. Maher, K. Edstrom, I. Saadoune, T. Gustafsson and M. Mansori, *Electrochim. Acta*, 2009, **54**, 5531.
8 O. Le Bacq and A. Pasturel, *Philos. Mag.*, 2005, **85**, 1747–1754.
9 B. Manoun, A. El Jazouli, P. Gravereau, J. P. Chaminade and F. Bourre, *Powder Diffr.*, 2002, **17**, 290–294.
10 B. Manoun, A. El Jazouli, P. Gravereau, J. P. Chaminade and F. Bourre, *Powder Diffr.*, 2003, **18**, 301–305.
11 S. Södergren, H. Siegbahn, H. Rensmo, H. Lindström, A. Hagfeldt and S. E. Lindquist, *J. Phys. Chem. B*, 1997, **101**, 3087.
12 B. Manoun, A. El Jazouli, P. Gravereau and J. P. Chaminade, *Mater. Res. Bull.*, 2005, **40**, 229.
13 T. Gustafsson, J. O. Thomas, R. Koksbang and G. C. Farrington, *Electrochim. Acta*, 1992, **37**, 1639.
14 J. Nordgren, G. Bray, S. Cramm, R. Nyholm, J.-E. Rubensson and N. Wassdahl, *Rev. Sci. Instrum.*, 1989, **60**, 1690.
15 C. Jung, F. Eggenstein, S. Hartlaub, R. Follath, J. S. Schmidt, F. Senf, M. R. Weiss, Th. Zeschke and W. Gudat, *Nucl. Instrum. Methods Phys. Res., Sect. A*, 2001, **467–468**, 485–487.
16 F. M. F. de Groot, J. C. Fuggle, B. T. Thole and G. A. Sawatzky, *Phys. Rev. B: Condens. Matter*, 1990, **42**, 5459.

17 A. Augustsson, M. Herstedt, J. H. Guo, K. Edström, G. V. Zhuang, P. N. Ross Jr, J.-E. Rubensson and J. Nordgren, *Phys. Chem. Chem. Phys*., 2004, **6**, 4185–4189.
18 A. Augustsson, A. Henningsson, S. M. Butorin, H. Siegbahn, J. Nordgren and J.-H. Guo, *J. Chem. Phys*., 2003, **119**, 3983.
19 L.-C. Duda, J. Downes, C. McGuinness, T. Schmitt, A. Augustsson, K. E. Smith, G. Dhalenne and A. Revcolevschi, *Phys. Rev. B: Condens. Matter*, 2000, **61**, 4186.
20 T. Schmitt, L.-C. Duda, A. Augustsson, J.-H. Guo, J. Nordgren, J. E. Downes, C. McGuinness, K. E. Smith, G. Dhalenne, A. Revcolevschi, M. Klemm and S. Horn, *Surf. Rev.Lett*., 2002, **9**, 1369.
21 T. Schmitt, L.-C. Duda, M. Matsubara, A. Augustsson, F. Trif, J.-H. Guo, L. Gridneva, T. Uozumi, A. Kotani and J. Nordgren, *J. Alloys Compd*., 2004, **362**, 143.
22 L.-C. Duda, T. Schmitt, J. Nordgren, P. Kuiper, G. Dhalenne and A. Revcolevschi, *Phys. Rev. Lett*., 2004, **93**, 169701.